京都大学防災研究所年報 第41号 B-2 平成10年4月
Annuals of Disas. Prev. Res. Inst., Kyoto Univ., No. 41 B-2, 1998

Wind-wave-current system in the nearshore zone

LU Ming*, Takao YAMASHITA, Toyoaki MISHIMA**

* Graduate School of Engineering, Kyoto University
** The NEWJEC Consultants, Inc., Japan

Synopsis

Coastal current in the nearshore zone is called nearshore current, which is mainly generated by breaking waves inside the surf zone together with winds in the wide area of the coastal zone. Both wind-induced currents and wave-induced currents are characterized by a shear-flow with a remarkable vertical distribution and complicated turbulence flow fields.

For mathematical molding of such nearshore currents, it is very important to make clear wind and wave stresses acting on the sea-surface. However, there have been no reliable observation of current profile inside the surf zone or information of wind stresses in the nearshore zone, because of its measuring difficulty without observation pier and advanced measuring instruments.

In this paper, we conducted a continuous measuring of nearshore current profile and wind stresses in/out the surf zone by using high frequency ADCP(Acoustic Doppler Current Profiler) installed on the sea-bottom under the observation pier(the T-shaped pier of Ogata Wave Observatory) together with ultra-sonic anemometer. This two-month observation unveiled a part of nearshore currents structure as well as wind drag coefficient in the nearshore zone.

Keywords: ADCP observation; nearshore current; wind stress; surf zone; current profile

1. Introduction

It has been recognized that beaches play an important role in the global environment. On the other hand, it has become to be a big social problem that the beaches disappeared due to human activity(beach erosion problem). For example, the shoreline retreat induced by the non-inverse offshore sediment transportation has been accelerated with the global sea level rise or extremely wave conditions. It is also conceivable that the width of beaches becomes smaller and smaller when the offshore sediment transportation accelerated by the storm waves together with changes in the grain size component of the sediment. Large sale beach changes was caused by imbalance of longshore sediment transport changes in wave and current fields and the effect of man-made structures, which affects not only beach changes but also natural environment such as water quality, the ecological system and natural resources.

Both in the United States of American and European countries, the usefulness of the beaches to the coastal environment as well as function of absorbing the impact of the waves (disaster prevention function) has been recognized in these several decades. Beach nourishment has been employed to recreate natural sand beaches instead of hard structures. The new research field, the so-called "Beach Engineering" has been developed, in which stable beach formation and maintenance, environmental and economic evaluation of beach formation have comprehensively been considered (Yamashita, 1997). The interdisciplinary studies for the coastal preservation will be developed in the field of beach engineering.

The prediction of beach changes is one of purposes of beach engineering. The external forces like winds, waves, ocean currents and nearshore currents make the sea bottom sediment move resulting in beach changes.

The numerical models for beach change prediction, therefore should consider to combine the models of the wave transformation, nearshore currents, sediment transport together with continuity of the sediment transport. Beach change prediction method can be classified into two types: one is the so called n-line model, the other is three-dimensional model. The n-line model estimates shoreline evolution by assuming the existence of equilibrium beach profiles, which is used for the beach change prediction of long term and extended domains. On the other hand, three-dimensional model is effective on predicting the sea bottom topography changes caused by local changes in waves and currents fields.

Numerical model of the beach changes, should be verified with the field observation, in which each models for waves, currents and sediment transport are examined independently or simultaneously. As the nearshore current model is the foundation of the beach change models, many types of nearshore current models have been developed and proposed. Within several decades, most of the nearshore current models have been developed as two-dimensional models, assuming the gradient of radiation stresses to be driving forces, in which the characteristics of the vertical distribution of the nearshore currents have not directly been taken into consideration. Although, three dimensional structure of the nearshore currents has recently been recognized, we have not enough knowledge to establish the three-dimensional mode. However, problems of computational capacity and heavy task make us stand with quasi three-dimensional models. Stive(1987) calculated the vertical distribution of the nearshore currents assuming the same distribution for longshore direction. Svendsen(1989) evaluated the longshore and on-offshore components form three-dimensional Navier-Stokes equations, and then estimated the nearshore currents by combining the components of longshore and on-offshore. Sanchez(1992) considered the return flow which obtained from experiment, estimated the nearshore currents with combining the horizontally two-dimensional and vertically one-dimensional models. Mellor(1996) employed the mode splitting method for three-dimensional nearshore current model.

On the other hand, for the case of the large scale of man-made coastal structures, or the remarkable changes in wave and current fields due to construction of coastal structures, we have to simulate their influences to the beach changes. It is also necessary to discuss more about the erosion control if we detect the remarkable topography changes by the simulation. However, because of the variety and complexity of the different conditions of beaches, it is difficult to get a universal result with enough accuracy by numerical simulation. For this case, we need the observation.

As almost all the remarkable beach erosions in the Japan's coasts facing Japan Sea have been caused by high waves and strong wind, so it is necessary to observe the waves, currents and sediment transport together with strong winds. Yamashita et al(1997) conducted a long term ADCP observations in this condition for elucidating the three-dimensional structure of nearshore currents by observation pier. They observed the vertical distribution of the nearshore currents in the surf zone to make clear as following: (1)The nearshore currents have almost uniform vertical distribution near the surf zone. (2) The nearshore currents is strongly influenced by the winds. It is also concluded from the observation that the characteristics of the waves, currents and turbulence in the shallow water under the condition of strong winds are very different from those in deep water.

Thus it is important to make clear the mechanism of momentum transfer from atmosphere to the sea near the surf zone(Watson, G. and Yamashita, T.1997). Wind-induced current may be equivalent to current induced by wave breaking in coasts facing the Japan Sea. When we establish a mathematical model for nearshore current, these effects should be taken into consideration.

A long term observations for winds, waves and currents under the high waves condition in winter in Ogata coast facing Japan Sea. ADCP observation was conduced along the observation pier of Ogata Wave Observatory, Disaster Prevention Research Institute of Kyoto University. The nearshore current profile against the external forces such as waves and winds was investigated. The wind stresses near the surf zone was also observed by three components ultrasonic anemometer and wind stresses are estimated by the Turbulence Dissipation Method (TDM) to formulate the wind drag coefficient against wind speed.

2. Observation of Nearshore Currents

Beach erosion due to offshore-going sediment transport is a serious problem for Japan's coasts facing Japan Sea. The mechanism of sediment transport to offshore has not yet been made clear. In this chapter, the winds, waves and currents system in the surf zone was observed at the T-shaped Observation Pier(TOP), Ogata Wave Observatory. Ultrasonic anemometer, ultrasonic 7 sets of wave gauges and high frequency ADCP (1200kHz, Workhorse Sentinel , RD Instrument) were used to make clear the nearshore current structure under the strong wind.

2.1 Observation System

The observation was conducted at the Ogata coast from March 2 to March 13, 1997 and from December 26 , 1997 to January 16, 1998.

(1) Wind and Wave Observations:

Wind was measured using a three component ultrasonic anemometer at 10m above the mean sea level. Seven ultrasonic wave gauges have been installed along the observation pier to measure wave direction (using a complete linear-array of 4 gauges, referred as ch1, ch2, ch3 and ch4 in Figure 1) and to measure wave attenuation due to breaking (using the 3 gauges : ch5, ch6 and ch7). Mean water level changes due to wave set-up and tides (about 0.3m) were also measured by the 7 gauges. The wave and wind data were observed for 20 minutes and 60 minutes, respectively, with the sampling frequency of 10Hz.

(2) Current Observations:

Two ADCP were installed on the sea bottom beneath the center of the two wings of TOP as shown in Figure 1. Beach profiles were also measured along the pier during and prior to the observation, in August, 1996 and March, 1997.

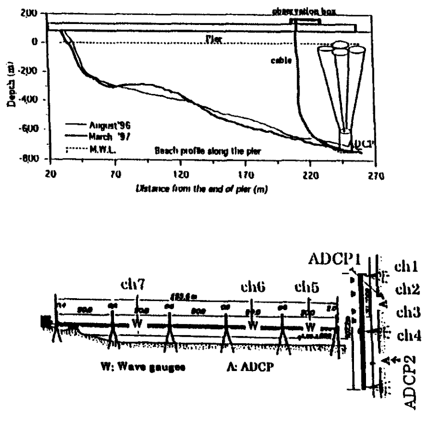

Figure1. Observation Pier and Equipment Set-up

2.2 Processing of ADCP Data

The main purpose of ADCP measurement is to know the velocity distribution of the nearshore currents in the surf zone. For this purpose, we changed the number of pings (1-30ping) and thickness of measuring layer (0.25m and 0.5m) to get the most suitable condition for wave and current observation. Consequently, the measuring mode of the ADCP was set to 8pings ensemble average (0.25sx8=2s sampling) for wave observation in 1997, and 30pings average for mean current observation in 1998, with 30 depth-cells of 25cm measuring layer. Data were continuously recorded and stored in MO disks. Tidal range of this region is smaller than 0.3m.

For mean flow detection, 2 and 6 minutes box averages were taken for data in 1997 and in 1998, respectively.

2.3 Nearshore Current Structure

2.3.1 Observations in 1998

Figure 2 shows the significant wave height and Figure 3 shows the time series of wind speed and direction, during the observation period. As the direction of shore-normal is north-west, wind from the north-west to south-west is referred as westerly wind, and wind from north-west to north-east is called easterly wind. From Figures 2 and 3, the highest wave and strongest wind occurred in the period of January 4 to 7.

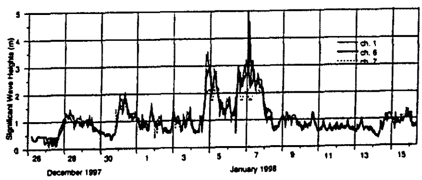

Figure2 Significant Wave Height
(26th,Dec,1997 to 16th,Jan,1998)

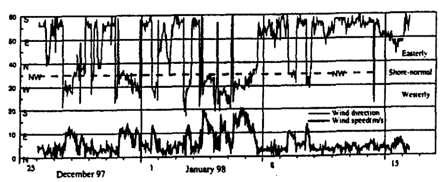

Figure3 Wind Speed and Wind Direction
(26th,Dec,1997 to 16th,Jan,1998)

Figure 4 shows time series of waves and winds after the westerly winds on January 4 (1:00pm,), in which a sharp increase of wave height is recorded (6:00pm) with the peak of wave period (8:00pm). These events may be correlated each other; as strong westerly winds generate wind waves and change their direction to be east with moving of meteorological dippression to the east, occurrence of wave period peak delays with several hours.

Figure 5 shows the off-shore currents in the observation period. The strong off-shore currents occurs suddenly. In order to investigate this sudden change of current against wind and wave conditions, winds and waves are plotted together in Figure 6, during 6:00am, January 6 to 8:00pm, January 7.

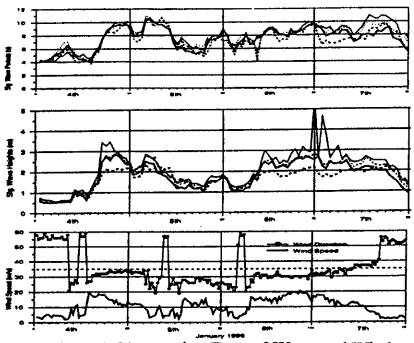

Figure4 Observation Data of Wave and Wind
(4th,Jan 1998 to 7th,Jan,19989)

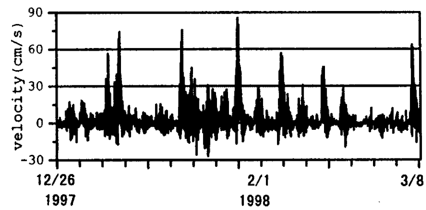

Figure5 Offshore Current Velocity
(26,Dec.1997 to 8,Mwr,1998)

Currents components of the on-offshore and longshore are plotted in Figures 6(c) and 5(d), respectively. Figure 6(a) indicates a drop of wave height at ch5 compared to ch4 at 8:00am, January 7. This can be interpret as an occurrence of wave breaking at some point between wave gauges ch4 and ch5 (20m onshore from ch4 as shown in Figure 1). In other words, the observation point moved from inside to outside the surf zone within the observation period depending on wind and wave conditions.

Furthermore, it can be observed from Figure 6(b) that the discrepancy between these wave gauges occurred when wind direction changed to easterly and wind speed became weak. Four storms, including the case shown in Figure 5, were observed in January and February, 1998. Analysis of other three cases are shown in Appendix, Figures. A1, A2 and A3, in which similar characteristics of currents, winds and waves were observed.

(a)Velocity Profile:

Figure 6(e) indicates that the remarkable offshore currents occur when the wind direction changes from westerly to easterly and there is no significant variation of velocity profiles both for longshore and offshore currents below the wave trough level.

(b)Longshore Currents:

Figure 6(c) shows that the longshore currents are strongly related with longshore components of the wind speed. Vertical distribution of longshore currents developed by strong winds is extremely stable and uniform. Note that the direction of the longshore currents fully depend on wind direction, i.e. westerly winds excite longshore currents going north-east and easterly winds produce longshore currents going to the south-west. Components of going offshore currents are much smaller than longshore components.

(c) Cross-Shore Currents:

Figure 6(d) shows that almost all currents below the wave trough level directs to offshore. When wind direction changes from westerly to easterly (shore-normal wind phase), a typical wind evolution pattern in the coasts facing the Japan Sea, strong offshore currents are observed. Vertical distribution of cross-shore current is characterized with strong shear flow which consists of on-shore going current above the trough level and off-shore going current below the wave trough.

2.3.2 Observation in 1997

Observation conducted in March, 1997 is shown in Appendix, Figure 7, in which the typical wave characteristics in the Japan Sea were recognized, i.e. the westerly winds generate wind waves coming from west, then wind direction changes to easterly with reducing wind speed. Swells from the north are observed after several hours from the peak wave height occurrence. When the wind direction changes to easterly, offshore currents become strong below the trough level, as similar to the observation in January, 1998.

3. Wind Stresses in Nearshore Zone

The stress factors represent the exchange of momentum between atmosphere and ocean, and between ocean and sea bed. Air-sea momentum exchange is a complex process involving turbulent boundary-layer flow over a changing rough surface, wave generation, non-linear energy transfer between wave components, and wave breaking. Waves also affect the bottom stress, by increasing bottom boundary layer turbulence and eddy viscosity, and hence

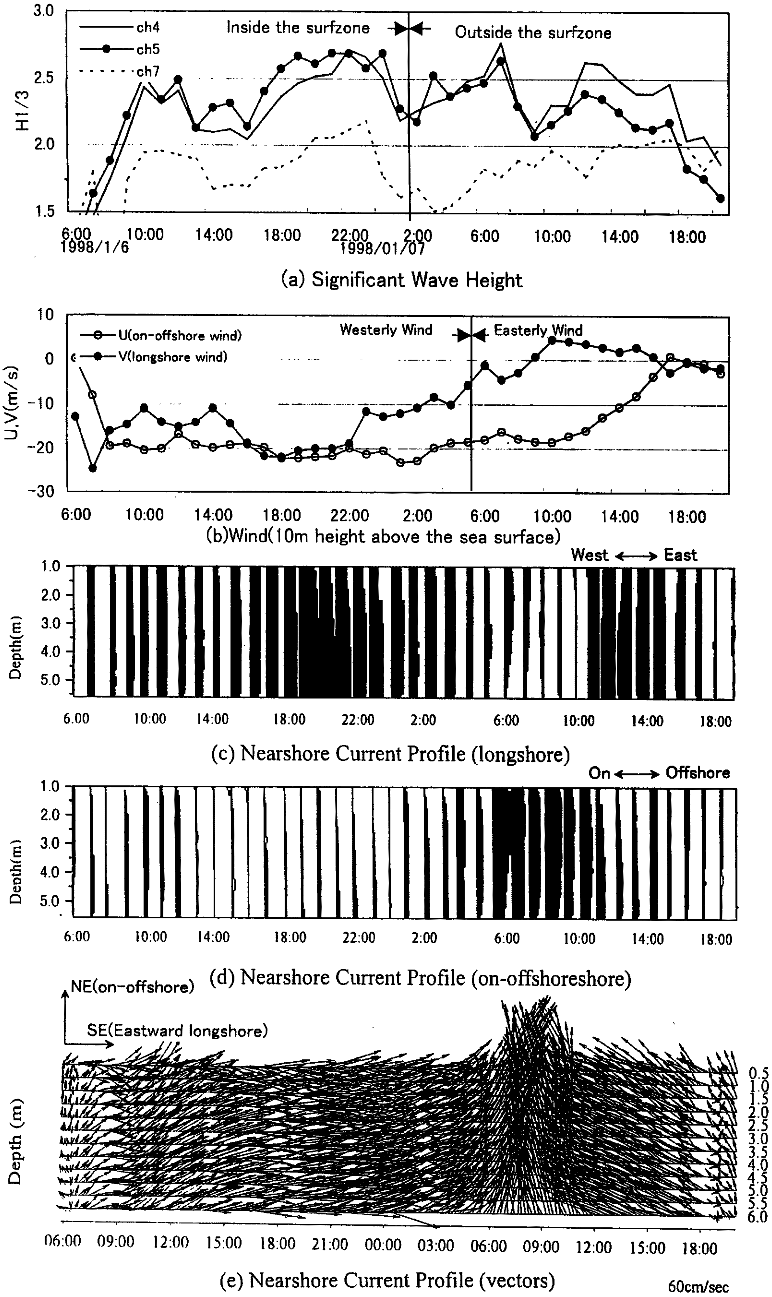

(a) Significant Wave Height

(b)Wind(10m height above the sea surface)

(c) Nearshore Current Profile (longshore)

(d) Nearshore Current Profile (on-offshoreshore)

(e) Nearshore Current Profile (vectors)

Figure6 Nearshore Current Profile against Wave and Wind (6,Jan.1998 to 7,Jan.1998)

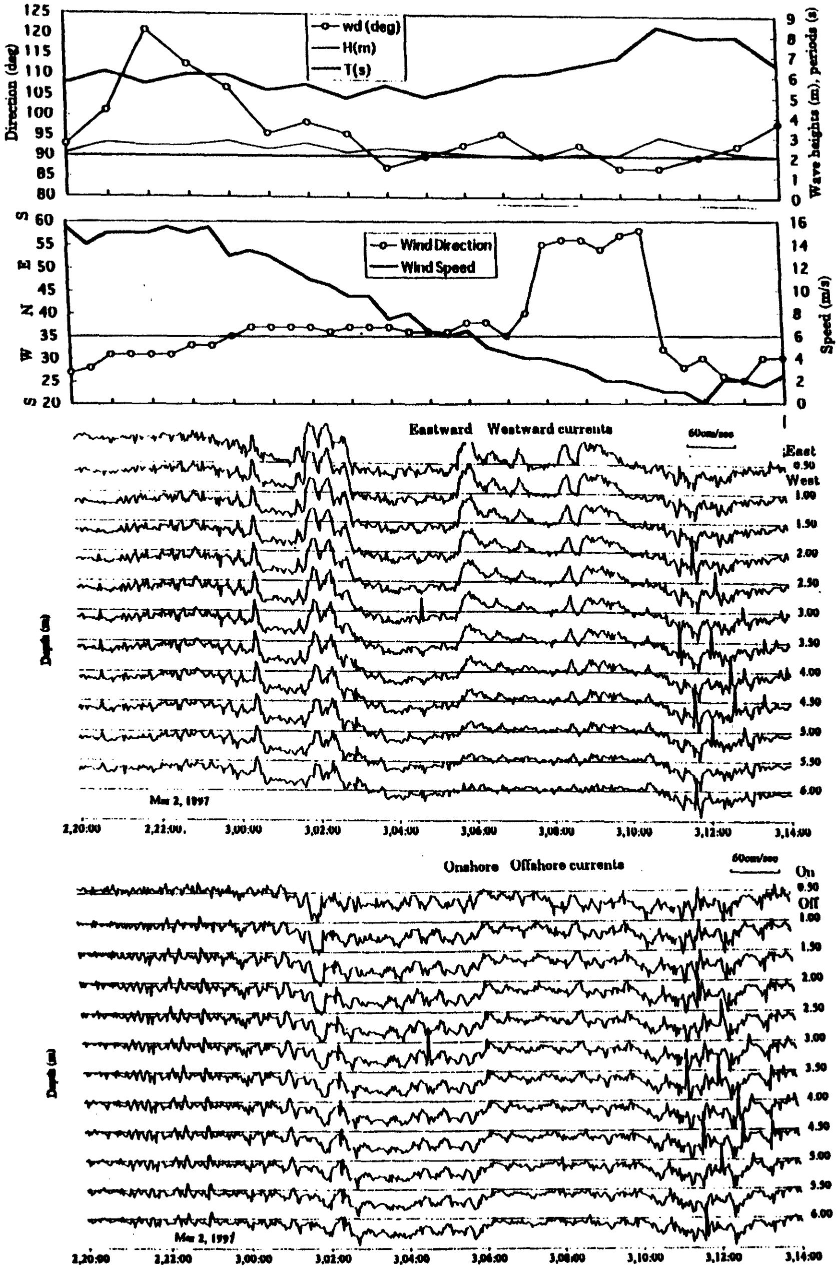

Figure7 Nearshore Current Profile against Wave and Wind (2,Mar.1997 to 3,Mar.1997)

momentum transfer. These processes are not very well understood theoretically, especially in strong winds and high waves, and so are not incorporated into the models. If they can be better understood, then in principle the accuracy of the corresponding forcing terms in the current models could be improved.

The wind turbulence was measured by a three-component ultrasonic anemometer, which is located on the top of the observation pier, at the height of 10m above mean sea level. Wind data were continuously recorded with 10Hz sampling and analyzed by the turbulent dissipation method (TDM) mentioned below.

3.1 Turbulence Dissipation Method

Following Yelland et al.(1996), wind stress was estimated from the anemometer data by using TDM which is based on the assumption that the energy spectrum of the down-wind component is governed by the rate of dissipation of energy caused by high frequency turbulence. In this case, the spectrum is assumed to have the form:

$$S(f) = K\varepsilon^{2/3} f^{-5/3} \left(\frac{U}{2\pi}\right)^{2/3} \qquad (1)$$

where $S(f)$ is the power spectrum of the down-wind component, K the 1-D Kolmogorov constant, taken to be 0.55, ε the high-frequency turbulent dissipation rate, U the wind speed. If the measured spectrum is found to obey the $f^{-5/3}$ law reasonably well, then an average value of $S(f)f^{-5/3}$ over an appropriate frequency range may be used in Eq.(1) to estimate ε. The wind stress τ is then estimated by

$$\tau = \rho_a (k_v \varepsilon z)^{2/3} \qquad (2)$$

where k_v is the von Karman constant which is taken as 0.4, and z is the measurement height (10 m).

The mean force acting on the surface of a body of water due to wind stress is usually approximated as:

$$\bar{\tau}_s = \rho_a C_{D10} \bar{U}_{10} |\bar{U}_{10}| \qquad (3)$$

where $\bar{\tau}_s$ is the wind stress at the surface, ρ_a the air density, $\bar{U}_{10}$ the mean wind speed at 10 m above the mean water level and C_{D10} the drag coefficient for wind at 10 m. To represent the fact that surface roughness increases with wind speed, this coefficient is normally specified as a function of the wind speed at 10m, as $C_{D10}(\bar{U}_{10})$.

The drag coefficient then can be obtained from Eq.(3) after correcting the observed mean wind speed to an estimated value at 10m above the mean sea level.

3.2 Wind Shear Formulation

The observation data are classified into four types by the wind direction as shown in Figure 8, Figure 9. They show the relation between the drag coefficient and wind speed which is taken to the 10 minutes average for each type.

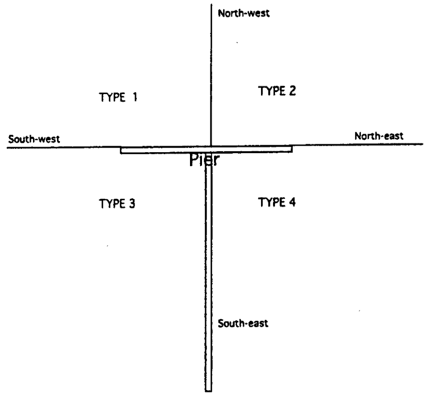

Figure8 Four Type of the Wind Direction

Figure 9 show that the wind from south-west to north-east (Figure 9a) is much stronger than that from the other direction , whose maximum value is about 24m/s. Almost all wind stronger than 10m/s are from this direction. When the wind speed of type 1 exceeds 10m/s , the relation between the drag coefficient and

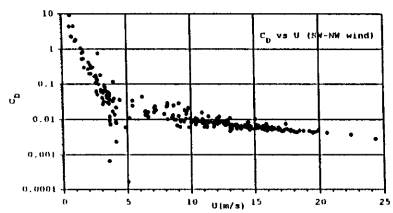

Figure9a Drag Coefficient Estimates against Wind Speed (tyre1)

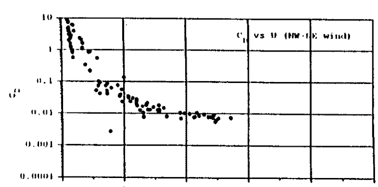

Figure9b Drag Coefficient Estimates against Wind Speed (tyre2)

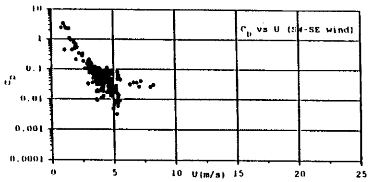

Figure9c Drag Coefficient Estimates against Wind Speed (tyre3)

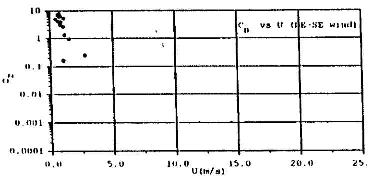

Figure9d Drag Coefficient Estimates against Wind Speed (tyre4)

average wind speed becomes to the following fitting curve as shown in Figure 10.

$$C_D = 0.0223\left(\frac{10}{3}\right)^{-\frac{U}{15}} \quad (4)$$

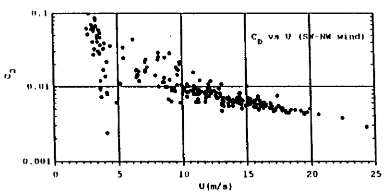

Figure10 Drag Coefficient Estimates against Wind Speed

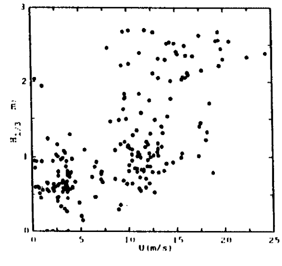

Figure11 Significant Wave Height against Wind Speed (tyre1)

The drag coefficient usually increases with wind speed in the ocean, however, drag coefficient near the surf zone shows opposite tendency as shown in Figure 9, and Figure 10 shows the significant wave height does not depend on the wind speed. It may be considered that the wave breaking reduce the roughness near the surf zone when wave heights increase.

4. Conclusions

In this study, we conducted a continuous measuring of nearshore current profile and wind stresses in/out the surf zone by using high frequency ADCP installed on the sea-bottom under the observation pier together with three-component ultrasonic anemometer. This two-month observation unveiled a part of nearshore currents structure as well as wind drag coefficient in the nearshore zone which are summarized below.

As a nearshore current structure:

1) Remarkable offshore currents occur when the wind direction changes from westerly to easterly and there is no significant variation of velocity profiles of both longshore and offshore currents below the wave trough level.

2) Longshore currents are strongly related to longshore components of the wind speed. Vertical distribution of longshore currents developed by strong winds is extremely stable and uniform.

3) The direction of the longshore currents strongly depends on wind direction

4) Components of offshore currents are much smaller than longshore components.

5) Vertical distribution of cross-shore current is characterized with strong shear flow which consists of on-shore going current above the trough level and off-shore going current below the wave trough.

As wind stresses near the surf zone:

1) Winds from south-west to north-east are much stronger than those from the other directions in this coast. 2) The relation between the drag coefficient and average wind speed becomes to the following fitting curve

$$C_D = 0.0223\left(\frac{10}{3}\right)^{-\frac{U}{15}}$$

when the wind speed exceeds 10m/s.

3) Drag coefficient near the surf zone shows opposite tendency as drag coefficient in the ocean. It may interrupt that the wave breaking reduce the roughness near the surf zone when wave heights increase.

Acknowledgments

The authors would like to extend their thanks to Mr. Kiyoshi Uchiyama, technician in Ogata Wave Observatory, for his kind help in observations.

This study was funded by the Ministry of Education, Science, Sports and Culture of Japan as the Research Project, grant-in-aid for Scientific Research (1997-1998), No.09555157, (the chief researcher, T. Yamashita, Kyoto University). Support for a part of observation was also received from the NEWJEC Consultants Inc. for verification of numerical models of nearshore circulation.

References

Yamashita, T., Tsuchiya, Y., Basco, D. R. (1997): Mutual evaluation of beach preservation methods in Japan, USA and EU. *Proc.of 44th Japanese Conf.on Coastal Eng*.pp691-695.

De Vriend. H. J. and Stive, M. J. F. (1987): Quasi-3D modelling of nearshore currents. *Coastal Eng*, Vol.11, pp.556-602,

Svendsen, I. A・.Lorenz, R. S. (1989) : Velocities in combined undertow and longshore currents, *Coastal Eng*., Vol.13,pp.55-79.

Sanchez, A., Collado, F. and Rodriguez, A. (1992): Vertically varying velocity field in Q-3D nearshore circulation. *Coastal Eng*, Vol.3,pp2811-2824,

Mellor (1996): Users guide for a three-dimensional, primitive equation, numerical ocean model.

Yamashita, T., Yoshioka, H., Lu, M., Kawaike, K. (1997): ADCP observation of nearshore current structure in the surf zone *Proc.of 44th Japanese Conf.on Coastal Eng*.pp361-365.

Yelland,M.J et al (1996): The use of the inertial dissipation technique for shipboard wind stress determination . J.Atmos. *Oceanic Technology*,11, pp1093-1108.

Watson, G., and Yamashita, T. (1996): Nearshore, wave and topographic effects in storm surges. *Coastal Eng*,Vol.2,pp.1417-1430.

Appendix

Three other cases of wind, wave and current profile observation in January and February, 1998 are shown below.

要旨

本研究では，日本海中部に位置する大潟波浪観測所の観測桟橋を援用し，ADCPによる海浜流の鉛直分布の長期間連続観測および超音波式風速計による海上風の乱流特性の観測を行った．この観測により，冬季の強風・高波浪時の砕波帯における流れの３次元構造と，それに及ぼす強風および波浪の影響について検討を行った．さらに，砕波帯近傍で強風により発生するせん断応力の評価方法を提案した．

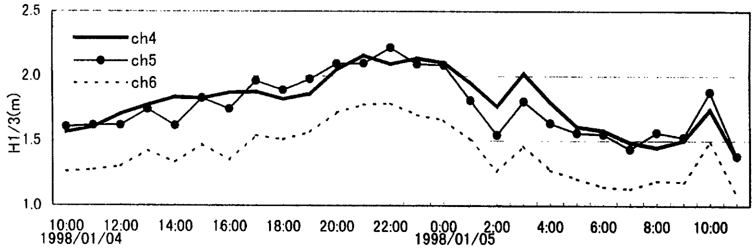

(a) Significant Wave Height(ch4,ch5.ch6)

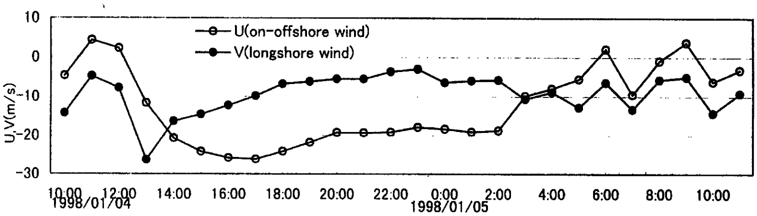

(b) Wind (10m height above the sea surface)

(c) Nearshore Current Profile (longshore)

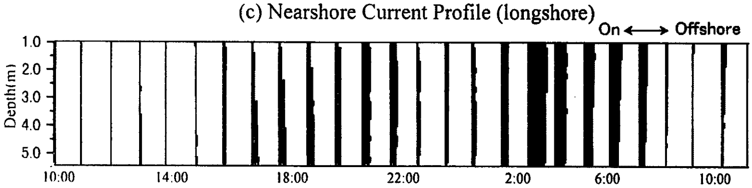

(d) Nearshore Current Profile (on-offshoreshore)

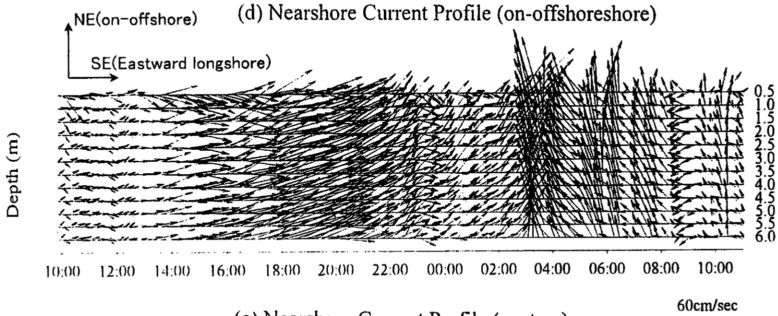

60cm/sec

(e) Nearshore Current Profile (vectors)

FigureA1 Nearshore Current Profile against Wave and Wind (4,Jan.1998 to 5,Jan.1998)

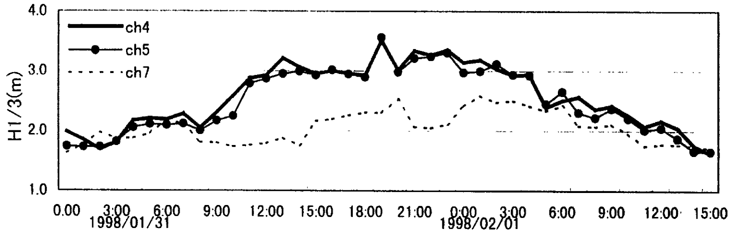

(a) Significant Wave Height(ch4,ch5.ch7)

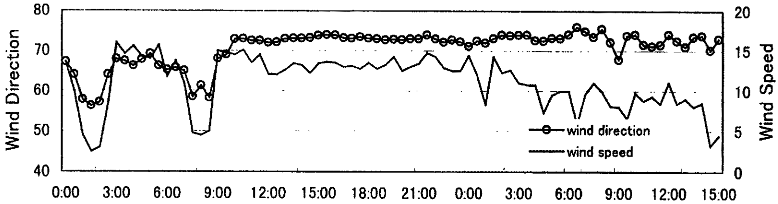

(b) Wind Speed and Wind Direction

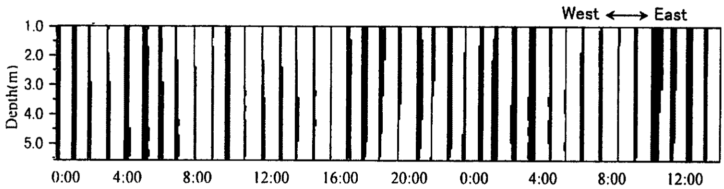

(c) Nearshore Current Profile (longshore)

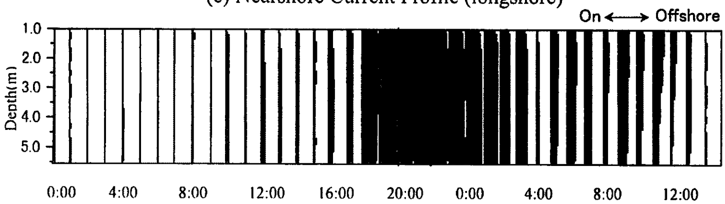

(c) Nearshore Current Profile (on-offshore)

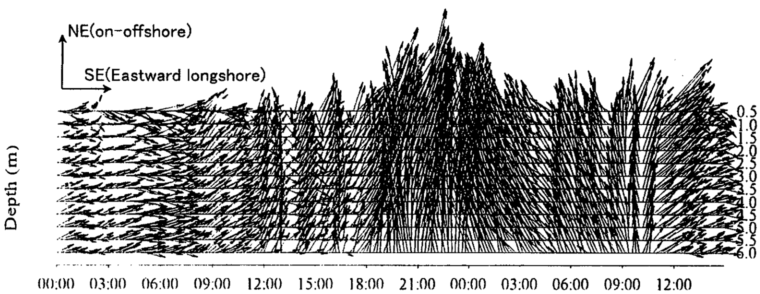

(e) Nearshore Current Profile (vectors)

FigureA2 Nearshore Current Profile against Wave and Wind (31,Jan.1998 to 1,Feb.1998)

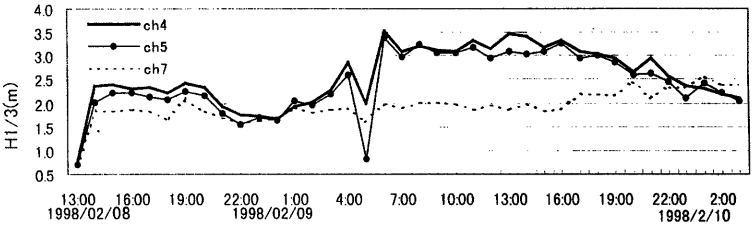

(a) Significant Wave Height(ch4,ch5.ch7)

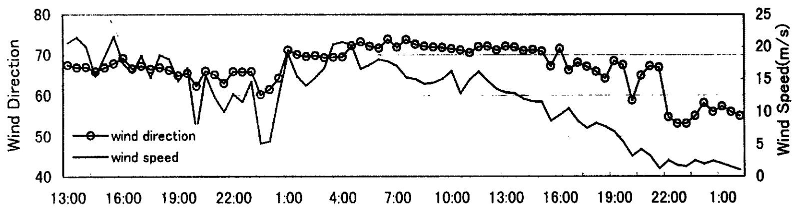

(b) Wind (10m height Above the surface)

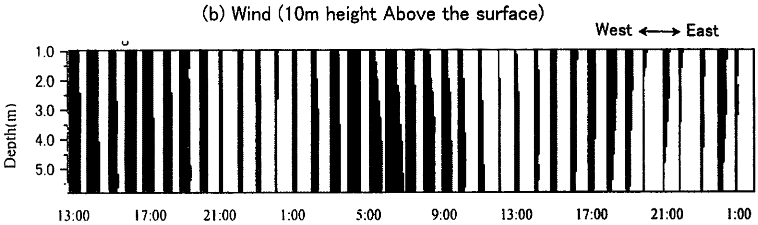

(c) Nearshore Current Profile (longshore)

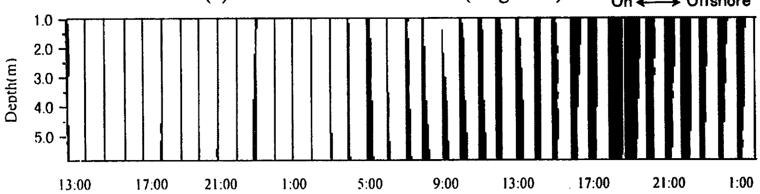

(d) Nearshore Current Profile (on-offshore)

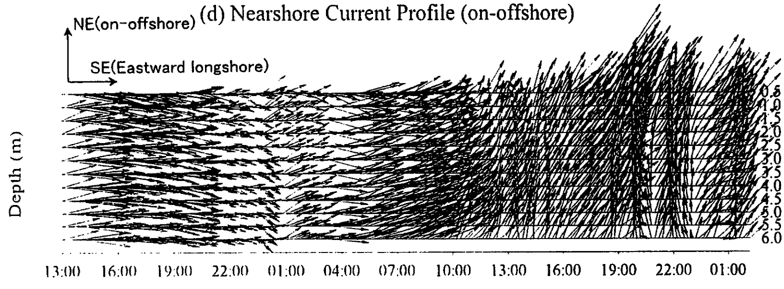

(e) Nearshore Current Profile (vectors)

FigureA3 Nearshore Current Profile against Wave and Wind (8, Feb.1998 to 10, Feb.1998)